







The expansion of land plants during the Late Devonian contributed to the marine mass extinction

Matthew S. Smart ^{1,2✉}, Gabriel Filippelli ¹, William P. Gilhooly III ¹, Kazumi Ozaki ³, Christopher T. Reinhard ⁴, John E. A. Marshall ⁵ & Jessica H. Whiteside^{5,6}

The evolution and expansion of land plants brought about one of the most dramatic shifts in the history of the Earth system — the birth of modern soils — and likely stimulated massive changes in marine biogeochemistry and climate. Multiple marine extinctions characterized by widespread anoxia, including the Late Devonian mass extinction around 372 million years ago, may have been linked to terrestrial release of the nutrient phosphorus driven by newly-rooted landscapes. Here we use recently published Devonian lake records as variable inputs in an Earth system model of the coupled carbon-nitrogen-phosphorus-oxygen-sulfur biogeochemical cycles to evaluate whether recorded changes to phosphorus fluxes could sustain Devonian marine anoxia sufficient to drive mass extinction. Results show that globally scaled increases in riverine phosphorus export during the Late Devonian mass extinction could have generated widespread marine anoxia, as modeled perturbations in carbon isotope, temperature, oxygen, and carbon dioxide data are generally consistent with the geologic record. Similar results for large scale volcanism suggest the Late Devonian mass extinction was likely multifaceted with both land plants and volcanism as contributing factors.

¹Department of Earth Sciences, Indiana University Purdue University Indianapolis, 723 W. Michigan St, Indianapolis, IN 46202, USA. ²Department of Ocean and Atmospheric Sciences, United States Naval Academy, 572C Holloway Rd, Annapolis, MD 21402, USA. ³Department of Earth and Planetary Sciences, Tokyo Institute of Technology, 2-12-1 Ookayama Meguro-ku, Tokyo 152-8551, Japan. ⁴School of Earth and Atmospheric Sciences, Georgia Institute of Technology, Atlanta, GA, USA. ⁵School of Ocean and Earth Science, University of Southampton, European Way, Southampton SO14 3ZH, UK. ⁶Present address: Department of Earth and Environmental Sciences, San Diego State University, 5500 Campanile Drive, San Diego, CA 92182, USA. ✉email: matt.smart@icloud.com

The Late Devonian mass extinction (also called the Frasnian–Famennian extinction and alternatively the Kellwasser Event, terminating at 372 Ma) is one of the “Big Five” Phanerozoic biotic crises^{1,2}. It is characterized by two distinct episodes of widespread marine anoxia^{3,4} expressed in the sedimentary record by the deposition of distinct black shale horizons^{3–5}. This marine biotic crisis is largely thought to have occurred in two distinct pulses, the earliest being the Lower Kellwasser (LKW) and the latter the Upper Kellwasser (UKW). Both pulses are associated with sizeable global carbon cycle perturbations, with positive carbon-isotope excursions ($\delta^{13}\text{C}$) ranging up to 4‰ reported in numerous studies in both carbonates and bulk organic matter^{4–7}. The development of sustained marine anoxia is linked to the demise of bottom-dwelling marine species^{3,8,9}, and it is also thought that water column oxygen depletion played a direct role in the catastrophic collapse of Devonian reef ecosystems^{2,10}. Proposed mechanisms for the Late Devonian extinction have included a wide range of hypotheses which include ultimate triggers such as astronomical forcing^{11,12}, bolide impacts^{13,14} and large igneous province (LIP) eruptions or similar large regional events^{15,16}, to proximate causes such as climate perturbations (both warming and cooling^{17–21}), enhanced terrestrial weathering associated with mountain building^{22,23} and the evolution and expansion of land plants^{24–26}. Despite the lack of agreement on ultimate causes and proximate (or resultant) triggers, a commonality amongst many of these competing theories is excess nutrient influx either from elevated terrestrial input or marine upwelling^{4,26,27}.

Global biogeochemical perturbations associated with the Late Devonian extinction have been widely reported (i.e., global positive $\delta^{13}\text{C}$ excursions). Numerous investigations into the geologic record across the KW events revealed additional global trends which exist independent of extinction ascription, such as a precipitous decline in atmospheric CO_2 ^{28–31}, a rise in atmospheric O_2 to near modern levels^{31–34} and cooling associated with each of the Kellwasser events³⁵. Given the wealth of information in the geologic record, the question arises as to whether global biogeochemical cycling supports any of these theories regarding the causal factor (or factors) driving the Late Devonian extinction.

Extinction mechanisms. While the various theories listed above have each been used to explain the Late Devonian extinction, it is prudent to first discuss some of the theorized mechanisms. Extinction mechanisms can be divided into two general categories, the ultimate causes and their resultant impacts on Earth’s surface, or proximate causes^{36,37}. For example, large scale volcanism has been implicated in many extinction events, however it is generally not volcanism itself which is the ultimate kill mechanism, but rather the eruption volume and the resultant effects on global temperature and atmospheric composition. In the case of the eruption of extensive areas of flood basalts or LIPs, both their size (which can range up to several million km^3) and their duration (generally less than one million years) make them ecologically significant. While the eruption of LIPs are most commonly associated with extinction level events, regional arc volcanism and submarine volcanism can also induce ecological stress, but may leave only a regional footprint in the geologic record or sometimes no footprint at all in the case of submarine volcanism which would be neatly erased through eventual subduction^{15,16,38}. Eruptions of LIPs or regional arc volcanism produce both short and long-term effects, the severity of each ultimately depending on the size and duration of the eruption (or series of eruptions as is often the case). Short-term cooling results from the production of sulfate aerosols which block incoming solar radiation. This is commonly referred to as “volcanic winter”

and lasts only one to two years, on average and depending on the severity of the eruption as mentioned above, as the sulfate aerosols are rapidly removed by rainfall. This cooling effect may be prolonged during LIP eruption, but is not likely to induce substantial climate change³⁶. Importantly, aside from being short-lived, this cooling effect is also self-limiting as the size of sulfate aerosols generally decreases as more sulfur dioxide is erupted³⁶. The more substantial and long-term impact from LIP eruptions is increased atmospheric CO_2 concentrations. As CO_2 is emitted rapidly and sequestered only over the course of geologic time via weathering, organic matter burial and photosynthesis, this effect is compounding the longer the eruption^{16,36}. The immediate impact of increased atmospheric CO_2 concentrations is an increase in global temperatures. A secondary impact of increased atmospheric CO_2 concentrations is ocean deoxygenation^{16,36}. Warmer water holds less dissolved oxygen. Additionally, warmer temperatures are generally associated with increased rates of precipitation. Increased precipitation enhances the runoff of terrestrial nutrients into oceans, which results in the bloom of primary producers such as plankton^{16,24,26,36}. The decomposition of organic matter in the ocean utilizes dissolved oxygen, thus plankton blooms will supply additional organic matter to the ocean bottom, ultimately decreasing dissolved oxygen concentrations³⁶. A large LIP eruption could result in a high enough atmospheric CO_2 concentration to drive widespread ocean anoxia, such as that which occurred during the end-Permian extinction³⁹.

Although the end-Permian extinction was a direct result of LIP eruption³⁹, not all LIPs are large enough nor ecologically catastrophic to produce mass extinction. This was most effectively demonstrated by Arens and West⁴⁰ in the development of their press-pulse extinction theory which contends that an environmental stress (press) such as the eruption of LIPs can be ecologically damaging due to its sustained duration, but must generally be followed by an additional catastrophic event (pulse) to produce broad extinction. While it is possible for LIPs to produce both press and pulse disturbances resulting in mass extinction such as in the end-Permian³⁷ and possibly the Triassic–Jurassic extinctions⁴¹ (two of the “Big Five” Phanerozoic extinctions), this should be considered the exception rather than the rule (Arens and West⁴⁰ find little correlation between extinction events in the Mesozoic and Cenozoic and LIP volcanism). Even so and as discussed above, as a sole kill mechanism the extinction power of LIPs lies in second order effects such as climate change and global carbon cycle disruption^{36,37,40}. Thus, to truly produce the theorized press-pulse response for an extinction such as the Late Devonian extinction (again, it is worth restating this is one of the “Big Five” Phanerozoic extinctions), LIP volcanism would have to be substantial indeed, and evidence for such an event would be expected to be found globally.

Of all the potential kill mechanisms, there is a growing body of evidence to support LIP eruptions as at least a contributing factor (primarily based on mercury enrichments and stratigraphic correlations, see refs. ^{15,16,42} and references contained therein). Three LIP eruptions occurred in the Late Devonian (Fig. 1b): the Viluy Traps in Siberia, the Kola LIP in the Kola Peninsula and the Pripjat–Dnieper–Donets (PDD) LIP in East Europe^{15,16}. Although current age estimates place the arguably smaller Kola and PDD LIPs loosely in the Late Devonian, the Viluy Traps have been much more closely associated with the Late Devonian extinction, having likely occurred in two distinct pulses at 374.5 ± 3.5 Ma and 363 ± 0.7 Ma^{43,44}, the former roughly coincident with the Frasnian–Famennian boundary. Given the potential ecological effects (specifically, ocean anoxia) discussed above and the existence of two distinct black shale horizons

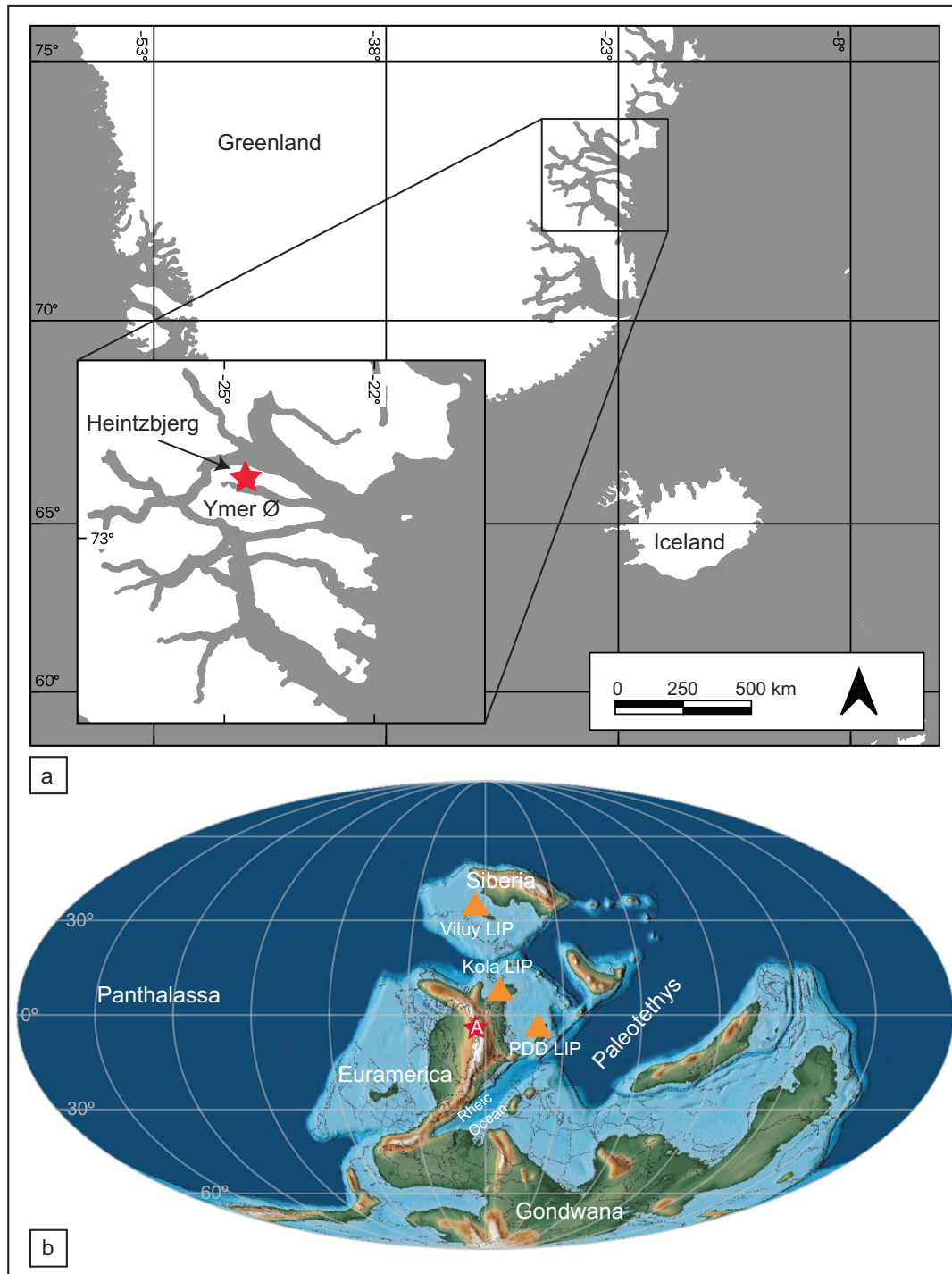


Fig. 1 Study location. **a** Location of the study site from which model data is derived (indicated by a red star). **b** Late Devonian (~370 Ma) paleogeographic reconstruction with the study location indicated by a red star as well as the relative locations of Late Devonian large igneous provinces (LIPs) indicated with orange triangles. LIPs include the Viluy LIP in Siberia, the Kola LIP in the Kola Peninsula and the Pripyat–Dnieper–Donets (PDD) LIP in East Europe. The base map was created using GPlates with reconstructions from ref. ⁸⁰. Locations of LIPs as described by Racki¹⁶.

concurrent with the Late Devonian extinction, the presence of at least one (and possibly more) LIPs in temporal proximity to the Late Devonian extinction offers a compelling possibility that large scale volcanism had some impact on biogeochemical cycling, and may have played a role in contemporaneous mass extinction.

Concurrently in the Late Devonian, land plant evolution reached a zenith as the earliest trees with substantial root systems,

such as *Archaeopteris*, achieved hegemony by the late Famennian^{45–47}. The development of root systems was a critical biologic innovation which subsequently enabled land plants to spread and colonize continental interiors, where previously their limited root systems confined them to areas immediately adjacent to bodies of water^{24,25}. It is this geologically rapid colonization that has been inferred to contribute in numerous extinctions of

varying severity from the Mid to Late Devonian^{24–26}. Prior to colonization by land plants, continental interiors were relatively unweathered, with vast amounts of the nutrient phosphorus confined to the mineral phase^{24–26}. Upon colonization, young landscapes were rapidly weathered in the nascent stages of soil formation, releasing large amounts of phosphorus which was eventually transported to Devonian oceans^{24–26}. This flush of nutrients would have a similar effect as that of large scale volcanism, stimulating a bloom in primary producers in the ocean leading to an increase in accumulation of organic matter and subsequent decrease in dissolved oxygen^{24–26}. On a global scale, this sudden and substantial nutrient influx could have been sufficient to drive widespread anoxia^{24–26}. While ocean anoxia does not always result in mass extinction, it proved catastrophic in the Late Devonian^{2,3,8–10}.

Large scale volcanism and enhanced terrestrial nutrient export and their connection to the Late Devonian extinction have been the subject of much debate (e.g., refs. 15,16,20,21,23,27,42,48,49). Both extinction mechanisms are rooted in events which are known to have occurred in the Late Devonian (i.e., there are three known temporally proximal LIPs^{15,16} and deeply rooting plants such as *Archaeopteris* also proliferated^{45–47}). These tectonic and biotic events potentially influenced global geochemical cycles, each leaving their own forensic footprint in the geologic record. Here we investigate the global geochemical impact of each of these events by utilizing new lacustrine records of phosphorus accumulation rate changes and employing an Earth system box model to simulate the carbon, nitrogen, phosphorus, oxygen and sulfur biogeochemical cycles. We explore both pulses of the Late Devonian extinction to determine whether large scale volcanism and its associated feedbacks or the expansion of deeply rooting land plants could plausibly result in the observed geochemical changes recorded in the rock record.

Enhanced phosphorus export during the Late Devonian mass extinction. The role of land plants in Devonian biotic crises has long been a subject of debate. As proposed by Wilder⁵⁰ and later refined by Algeo et al.²⁴, the expansion of land plants into continental interiors along with the development of large and complex root systems and arborescence led to an unprecedented flux of terrestrial nutrients into Devonian seas. The relatively large and geologically rapid nutrient load would have stimulated primary productivity leading to eutrophication, elevated organic matter deposition and subsequent bottom water anoxia. Occurring on a large enough scale, this could drive widespread marine anoxia, something which was relatively common throughout the Devonian^{24,26}. Until recently however, no studies have focused on quantifying a potential terrestrial nutrient pulse from land plant expansion by interrogating weathering-proximal terrestrial lacustrine records. Smart et al.²⁶ conducted such a study and was able to establish a relational link between the colonization of deeply rooting land plants and multiple episodes of elevated terrestrial nutrient export from the Mid to Late Devonian. Two such pulses were identified in a fluvial sequence from Heintzbjerg in the Devonian Basin of East Greenland associated with the LKW and UKW (Fig. 2)²⁶. These and similar pulses discovered earlier in the Devonian are accompanied by macro and microfossil evidence of the progymnosperm *Archaeopteris*, thus establishing a causal link between the proliferation of deeply rooting land plants and elevated terrestrial nutrient export²⁶. In several cases, these nutrient export events were both substantial in magnitude and sustained in duration (lasting up to several hundred thousand years in some cases and coinciding with smaller marine anoxic events, such as the Kačák event in the Mid Devonian)²⁶, enabling their use in geochemical models. The

increases in phosphorus accumulation rates at Heintzbjerg²⁶ compare favorably to revegetation following glacial retreat in Holocene analogs, lending confidence in the utility of their data (Extended Data Table 1). Furthermore, the paleogeographic location of the Heintzbjerg study site was on the flanks of the Caledonian mountains and within a drainage basin that ultimately fed into the Rheic Ocean (Fig. 1). Thus, elevated nutrient export from this location likely had a direct impact on biogeochemical cycling within the Rheic Ocean.

Model description. In this study, we employ an Earth system box model of the coupled C-N-P-O₂-S biogeochemical cycles developed by Ozaki and Reinhard⁵¹. The basic model design is based on the Carbon Oxygen Phosphorus Sulfur Evolution (COPSE) model^{52,53}. The model includes a series of biogeochemical processes operating on the planetary surface but is abstracted enough to allow the simulations on geologic time scales (see *Methods* and *Supplementary Information*).

We investigate several different scenarios in which we explore biological and tectonic factors individually. First, we explore the possible impacts of enhanced phosphorus weathering by land plant colonization using both P/Al and phosphorus accumulation rate data from Heintzbjerg, Greenland. In the sensitivity experiments, discrete episodes of phosphorus weathering are assumed with different timing and amplitude. Sharp increases followed by decreases of phosphorus weathering are meant to represent possible phases of selective phosphorus weathering associated with land plant colonization and a subsequent drop due to the establishment of phosphorus recycling in soil systems⁵³. We also explore the impacts of variations in degassing rates from LIPs that were active during the upper Devonian (Fig. 1b). While the exact timing and magnitude of Devonian volcanic eruptions are difficult to constrain, Late Devonian mercury (Hg) records indicate enrichment relative to total organic carbon in multiple locations during both the LKW and UKW^{15,16}. Hg enrichment can be used as a proxy for large scale volcanism, but its application is not straightforward as Hg enrichments can be caused by other factors unrelated to volcanism (e.g., soil weathering, variations in sedimentation rate, etc) (see refs. 16,54 and references contained therein). However, a study by Kaiho et al.⁵⁴ compared Hg enrichments observed in several Devonian biotic crises to coronene, a polycyclic aromatic hydrocarbon associated with large scale volcanism and discovered a correlation between Hg and coronene during the LKW and UKW, concluding that volcanism was likely during both pulses⁵⁴. Thus, based on Hg records we simulate two episodes of large-scale volcanism, a smaller event at the onset of the LKW and a larger event at the onset of the UKW.

In the COPSE type model, the ocean-atmosphere system is treated as a single reservoir. Therefore, the model is only appropriate for timescales longer than the mixing time of the ocean. More specifically, processes such as the solubility pump and the impact of ocean circulation on biogeochemical cycles are beyond the scope of this model, and simulated atmospheric CO₂ levels could fail to capture variability on timescales of <~10 kyr.

In the original COPSE model (e.g., refs. 31,52), the ocean alkalinity balance was assumed (i.e., input flux of alkalinity equals the output flux via carbonate burial). In contrast, our model⁵¹ explicitly calculates the alkalinity budget in the ocean by evaluating the carbonate system. This approach enables us to assess the time evolution of seawater pH on timescales longer than 10 kyr.

Results and discussion

Results for the enhanced terrestrial nutrient export scenario are shown in Fig. 3. Several different scenarios are explored: red and

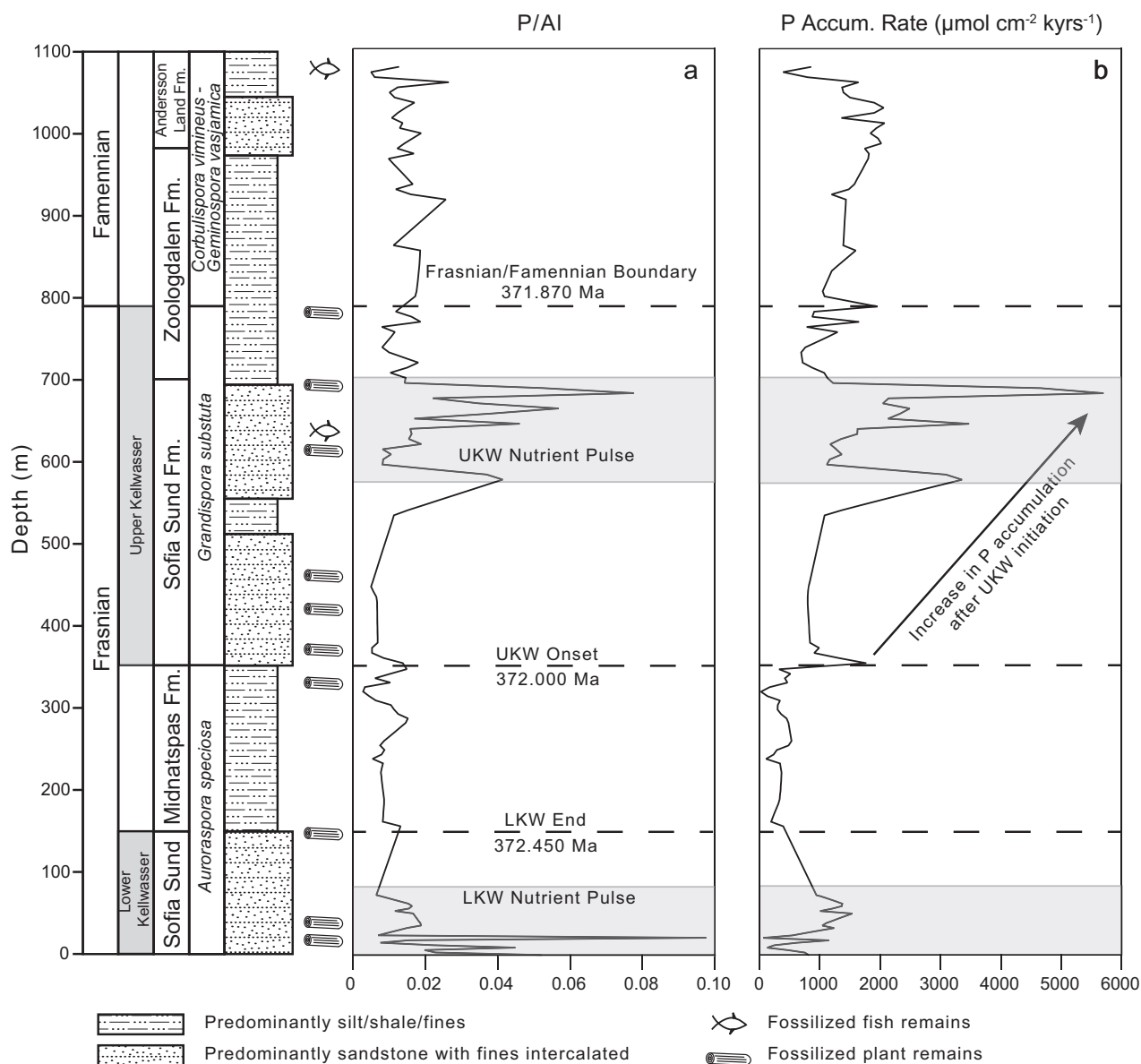


Fig. 2 Geochemical source data from the Heintzbjerg study location. The Heintzbjerg sequence contains 1100 m of continuous fluvial record capturing a portion of the Lower Kellwasser (LKW) as well as the entirety of the Upper Kellwasser (UKW) events comprising the Frasnian–Famennian extinction. Stratigraphy has been simplified due to the size of the sequence. The three distinct palynozones used for the relative placement of the Frasnian–Famennian boundary and the UKW are noted to the left of the stratigraphy^{69,70}. Black dashed lines represent the age control points used to calculate sedimentation rates based on recent age estimates^{11,27}. Shaded regions represent nutrient pulses during the LKW and UKW based on P/Al data²⁶. **a** Phosphorus/aluminum ratios used to estimate riverine phosphorus flux. Based on this data, two distinct nutrient pulses can be identified. **b** Phosphorus accumulation rate data calculated using estimated sedimentation rates based on cyclostratigraphy and used to simulate terrestrial phosphorus input in a separate simulation. These data show a greatly reduced nutrient pulse during the LKW and a large and sustained nutrient pulse during the UKW.

blue lines assume episodes with linear increases and decreases around the LKW and UKW, and the black line is obtained by scaling the P/Al (left panel) and phosphorus accumulation rate (right panel) records from Heintzbjerg, Greenland. Our model demonstrates the increase in riverine phosphorus flux, scaled from the Heintzbjerg data, promotes oceanic eutrophication and deoxygenation (as shown as increases in DOA, or degree of anoxia). For the LKW, the enhanced burial of organic matter in the ocean leads to a drop in atmospheric CO₂ levels (from ~10.5 present atmospheric level (PAL) to ~7.5–9 PAL) and associated climate cooling of 0.5–1.5 °C. This is accompanied with a positive excursion in δ¹³C of 1.5–3.0‰. These trends are observed in both the red/blue simulations as well as the scaled P/Al data from

Heintzbjerg (black line in Fig. 3). Also observed is that greater phosphorus weathering results in larger environmental changes. In the large linear simulation (blue line in Fig. 3), atmospheric O₂ levels exhibit a stepwise increase to the modern level of 21%. On the other hand, the sulfur isotopic value of seawater sulfate is largely insensitive to the variations of phosphorus weathering. Results based on the phosphorus accumulation rate data are similar, with a notable difference being the much smaller perturbations associated with the LKW.

Results for the enhanced volcanic degassing scenarios are shown in Fig. 4. A two-fold increase in degassing rate produces a positive excursion in δ¹³C (1‰) for the LKW, and a five-fold increase is required to produce the 2‰ excursion for the UKW.

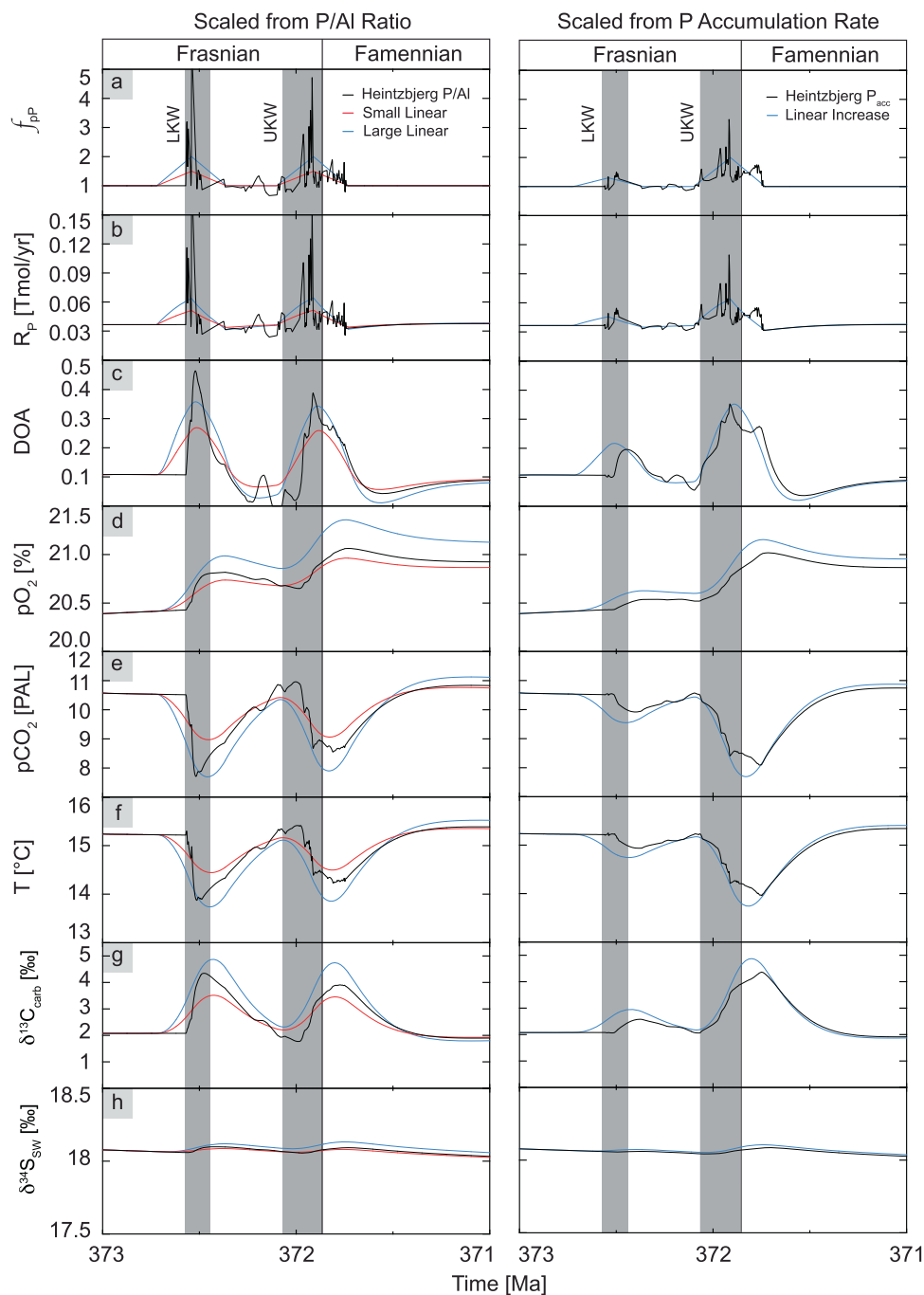


Fig. 3 Biogeochemical dynamics induced by elevated episodes of P weathering on land. Gray shaded regions represent the two pulses of the Kellwasser extinction. **a** Phosphorus weathering forcing factor, f_{PP} . Several different scenarios are explored: red and blue lines assume episodes with linear increase and decrease around the LKW and UKW, and black line is obtained by scaling the P/AI (left panel) and phosphorus accumulation rate (right panel) records from Heintzberg, Greenland. **b** Riverine P flux to the ocean. **c** Degree of oceanic anoxia. **d** Atmospheric O_2 level. **e** Atmospheric CO_2 concentration indicated as multiples of present atmospheric level (PAL). **f** Global average surface temperature. **g** Carbon isotopic value of burying carbonates. **h** Seawater sulfate sulfur isotope.

Such an enhanced volcanic flux during the UKW results in atmospheric CO_2 levels of >20 PAL and associated >4 °C increase in global temperatures. Under such conditions, an enhanced greenhouse accelerates terrestrial phosphorus weathering, promoting oceanic eutrophication and deoxygenation. This, in turn, leads to the enhanced burial of organic matter in marine sediments and a stepwise increase in atmospheric O_2 .

The terrestrial nutrient export scenarios and volcanic activity scenarios both demonstrate enhanced riverine phosphorus input flux, resulting in similar behaviors with respect to oceanic

biogeochemical dynamics (eutrophication, deoxygenation, and enhanced burial of organic matter) and the secular evolution of atmospheric O_2 levels. In contrast, these scenarios demonstrate different climatic variations. Specifically, the enhanced terrestrial nutrient export scenarios suggest a marked decrease in atmospheric CO_2 and global cooling of >1 °C whereas the enhanced volcanic activity results in the two-fold increase in atmospheric CO_2 levels and global warming of >4 °C. Additionally, while both scenarios achieve the positive $\delta^{13}C$ excursion recorded in the geologic record, the longevity of the excursions tends to be greater

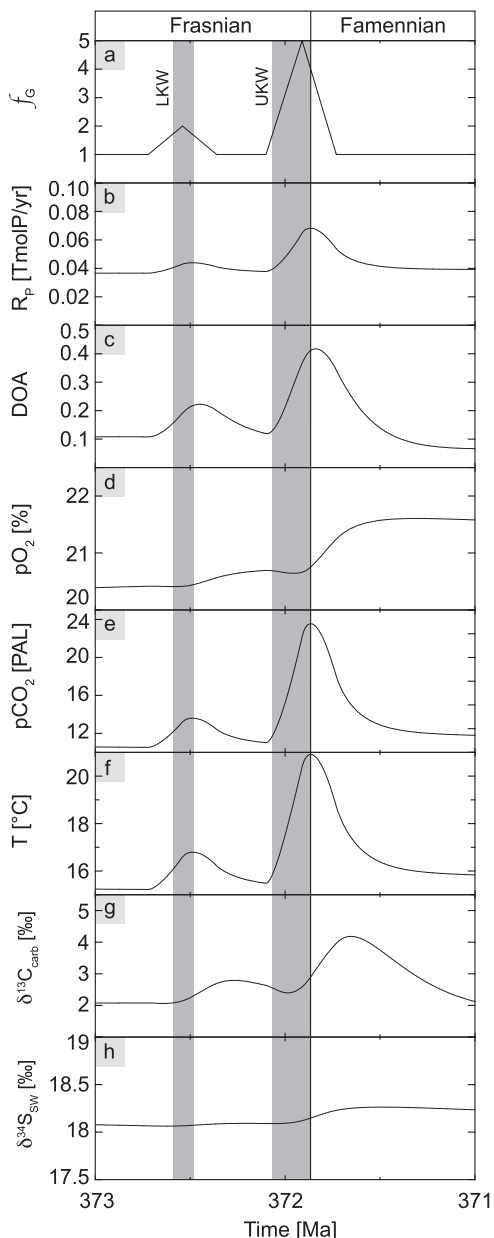


Fig. 4 Biogeochemical dynamics induced by enhanced volcanic activity.

Black line represents two distinct volcanic events, one during the LKW and a second during the UKW based on the presence of two distinct weathering events in the Heintzbjerg, Greenland data. Gray shaded region represents the two pulses of the Kellwasser extinction. **a** Degassing factor, f_{LIP} . **b** Riverine P flux to the ocean. **c** Degree of anoxia. **d** Atmospheric O_2 level. **e** Atmospheric CO_2 concentration indicated as multiples of present atmospheric level (PAL). **f** Global average surface temperature. **g** Carbon isotopic value of burying carbonates. **h** Seawater sulfate sulfur isotope.

in the enhanced volcanic activity scenario than those of the terrestrial nutrient export scenarios because of the increased residence time of inorganic carbon in the ocean-atmosphere system. Additionally, maxima in climate cooling in the enhanced terrestrial nutrient export scenario correspond to the largest positive excursion in $\delta^{13}C$, whereas in the enhanced volcanic activity scenario, the $\delta^{13}C$ excursion is delayed and occurs after the temperature maxima.

Both scenarios are somewhat at odds with the geologic record in differing respects. While an overall warming trend is observed through the Late Devonian, conodont oxygen isotope records

from numerous studies suggest cooling leading into both the LKW and UKW^{20,55,56} (although it is also worth noting that in some cases, cooling is reported as post-dating the onset of the $\delta^{13}C$ excursion⁶). If large scale volcanism (either from LIP or multiple arc volcanic events¹⁵) was an initiating mechanism, the enhanced volcanic activity scenario requires warming on a global scale (Fig. 4f) which is not supported by conodont oxygen isotope records. Additionally, atmospheric CO_2 decreased substantially throughout the Devonian. Our model predicts large scale volcanism sufficient to drive anoxia would have increased atmospheric CO_2 to levels which are likewise not supported in the geologic record. A compilation published by Franks et al.²⁹ compares Paleozoic CO_2 estimates from paleosol carbonates, fossil records and model estimates using GEOCARBSULF and reports a likely atmospheric CO_2 range of between 500–3000 ppm for the Late Devonian, substantially below >20 PAL required by our model (see also refs. ^{30,31}). Furthermore, values closer to the lower end of that range appear most likely based on a recent model of lycophyte leaf gas-exchange published by Dahl et al.⁵⁷ suggesting atmospheric CO_2 values of between 525–715 ppm for the Mid to Late Devonian. However, many of these records lack the temporal resolution to detect ephemeral perturbations, so although current evidence does not support rapid and dramatic increases in atmospheric CO_2 due to large scale volcanism it cannot be completely ruled out.

Our model results are more consistent with enhanced terrestrial nutrient export as an important proximate causal factor in at least the UKW extinction pulse as the predicted cooling, decrease in atmospheric CO_2 , and increase in atmospheric O_2 are all supported by the geologic record. The P/Al based model predicts larger geochemical perturbations during the LKW, which is inconsistent with most records that suggest the UKW was the more severe. This contrasts with phosphorus accumulation rate-based data which accurately predicts the UKW as the more severe event. Additionally, the similarities in geochemical response between the Heintzbjerg sequence and the linear simulations further reinforce the supposition that the terrestrial nutrient export model is the more likely of the two scenarios. However, the timing of the terrestrial nutrient pulses²⁶ seems to preclude plant expansion as an ultimate cause of extinction. Although there is evidence of elevated nutrient export during the LKW and at the start of the UKW, the most substantial and sustained nutrient export event occurs in the second half of the UKW, closer to the Frasnian–Famennian boundary (Fig. 2). While land plants may not have directly initiated the UKW, the concurrent extinction of both benthic species and the collapse of Devonian Reefs systems suggest the possibility of multiple extinction mechanisms. Rather than singular triggers, we suggest multiple elements of current theories contributed to biotic crises in the marine biosphere.

Comparison with global records. One of the inherent advantages to utilizing fluvial and lacustrine records to track terrestrial phosphorus export is their capacity to record local and basin-scale variations, which can more directly be compared with macro- and micro-fossil evidence of land plant activity, thereby establishing a causal link²⁶. Indeed, palynological records from Heintzbjerg support the presence of deeply rooting land plants such as *Archaeopteris*²⁶. Therefore, the Heintzbjerg site was chosen to drive inputs for the geochemical model utilized herein. The question arises however, can events at Heintzbjerg truly be representative of global trends and thus justifiably used to drive a global model? Unfortunately, similar but geographically distinct fluvial and lacustrine records do not yet exist for the late Frasnian, hindering efforts to further support the assertion that events at Heintzbjerg were indicative of global trends. However, there are a



Fig. 5 Geographic distribution of Late Devonian phosphorus records. Marine records (B–E) are shown in relation to the Heintzbjerg study site (A), indicated as red stars. Marine records include: (B) Steinbruch Schmidt, Germany; (C) Kowala, Poland; (D) Coumiac, France; and (E) H-32 Core, Iowa, USA. The Viluy large igneous province (LIP) is indicated by the orange triangle. The base map was created using GPlates with reconstructions from ref. ⁸⁰. Locations of LIPs as described by Racki¹⁶.

number of marine records which overlap and include both phosphorus data and cyclostratigraphic timescales like those employed here. Figure 5 notes the locations of four such records from several studies: Steinbruch Schmidt in Germany^{11,27}, Kowala Quarry in Poland^{27,58}, Coumiac in France²⁷ (this section lacks a cyclostratigraphic study, but includes a Global Boundary Stratotype Section and Point for the base of the Famennian) and the H-32 core in Iowa, USA^{58,59}. The section at Steinbruch Schmidt was deposited in a pelagic marine setting east of Euramerica⁶⁰ and contains distinct sedimentary expressions of both extinction pulses⁹. Kowala Quarry was deposited on a carbonate platform to the northeast of Euramerica and likewise contains sedimentary expressions of both extinction pulses^{27,58}. Coumiac represents a pelagic marine setting on the southeastern edge of the Rheic Ocean and also includes both extinction pulses²⁷. Finally, the H-32 core is sourced from the Illinois Basin, an epicontinental basin off the western coast of Euramerica, and includes sedimentary expression for the UKW only^{58,59}. Together, these four sites substantially expand the geographic range of phosphorus records with which the Heintzbjerg record can be compared.

Much like the study at Heintzbjerg by Smart et al.²⁶, all four sites include both P/Al and organic carbon to total phosphorus ratios ($C_{org}:P_{tot}$). While P/Al data can be informative of phosphorus flux relative to detrital input, $C_{org}:P_{tot}$ is a widely used paleoredox proxy and the combination of the two proxies can establish a causal relationship between elevated phosphorus input and any subsequent anoxia which develops (see refs. ^{23,26}). In the case of all four sites, periods of either anoxia or at least dysoxia are associated with the UKW interval (see refs. ^{23,27,59} and references contained therein). What makes all four sites compelling however, is that much like Heintzbjerg, each contain elevated values of phosphorus with respect to detrital input (P/Al) during the UKW (Fig. 6). Whilst the timing of the P/Al maxima during the UKW amongst the four sites is not synchronous, the magnitudes compare strikingly well to those at Heintzbjerg (Fig. 6). While variations in timing may at first glance seem contradictory, it is important to consider that land plant evolution and expansion was likely episodic, occurring at different times in distinct geographic regions²⁶. As noted by Smart et al., geographically punctuated phosphorus weathering events would be expected in order sustain or exacerbate large scale ocean anoxia²⁶. Moreover, enhanced terrestrial nutrient flux has been implicated directly as a driver for anoxia during the

UKW interval at Kowala²³ and indirectly in the Illinois Basin at the H-32 core⁵⁹ (although it should be noted that while there is no conclusive evidence linking enhanced terrestrial nutrient flux to anoxia at Coumiac and Steinbruch Schmidt²³, that possibility cannot be completely ruled out). While Smart et al. attributed the elevated influx of phosphorus at Heintzbjerg to the spread of land plants through the local basin, no such attribution exists for the other four sites described above. However, the presence of similar magnitude P/Al perturbations at all five sites during the UKW suggests a distinct geochemical similarity between them. The similar timing and magnitude may simply be circumstantial, but more likely it is indicative of broader scale trends impacting the basins surrounding Euramerica. It is on this basis that Heintzbjerg is deemed a suitable location from which to base the forcing factor for our geochemical model.

A multifaceted extinction mechanism. The Heintzbjerg sequence is a terrestrial equivalent to marine expressions of the KW events and is characterized by the deposition of two intervals of thick sandstones representing intense fluvial activity followed by stacks of palaeosols representing intense and prolonged intervals of aridity (see Fig. 2)⁶¹. These sedimentary markers suggest that the deposition of the UKW horizon at Heintzbjerg marks a defined shift in climate regimes from arid to warm and wet^{26,61}. Concurrent with this shift in climate regimes is evidence of elevated terrestrial phosphorus export (Fig. 2). Such a climate shift would bring about conditions generally more favorable for plant growth, potentially explaining enhanced terrestrial phosphorus export at the start of the UKW. Marine records from other sites report similar (and generally higher) rates of phosphorus export (Fig. 6), suggesting this scenario could indeed be a global one. Additionally, it is possible that at least one pulse of the Viluy Traps LIP (the largest Devonian LIP and the one which has been most closely associated with the Late Devonian extinction) occurred during the UKW^{16,42}. While precise timing of the other two LIPs discussed here prevent their definitive association with either of the KW events, it is possible that either or both played a role as well⁴². While our model predictions appear to rule out cataclysmic volcanism as a sole extinction mechanism, they do not discount it completely.

At the onset of the UKW, our model predicts substantial geochemical changes with increased terrestrial nutrient delivery driving positive $\delta^{13}C$ excursions, corresponding increases in O_2 and DOA as well as decreases in CO_2 and temperature. One

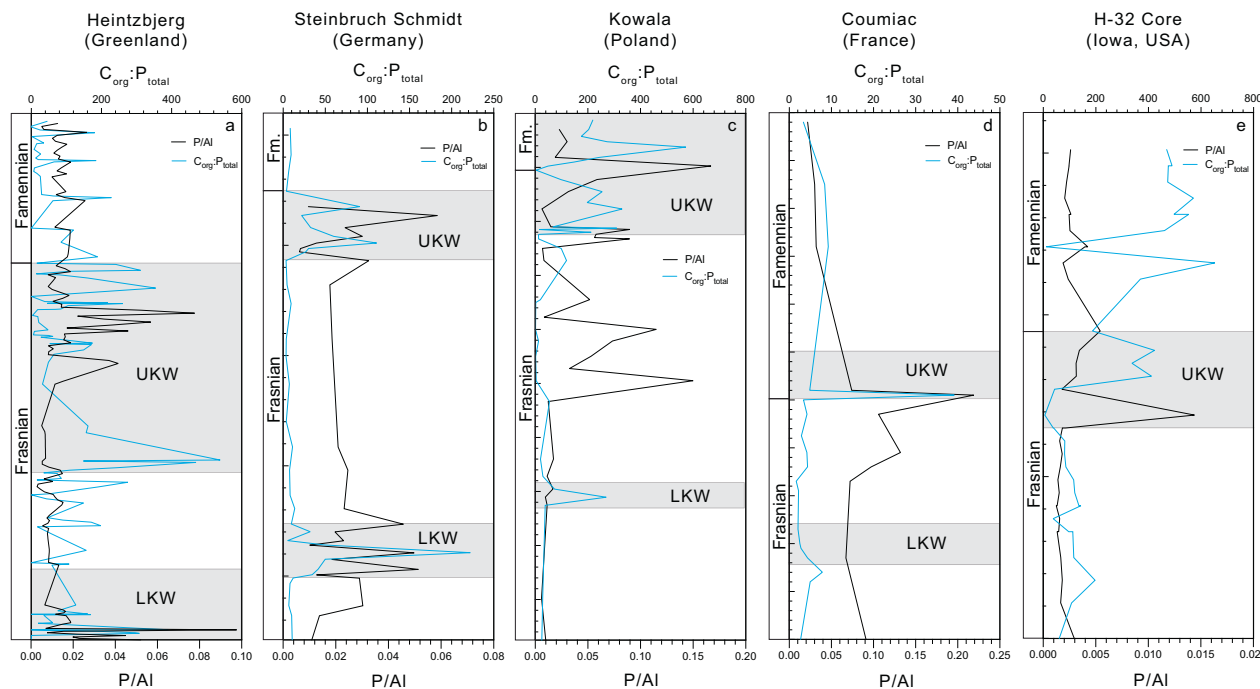


Fig. 6 Comparison of Heintzbjerg data to similar marine records. P/AI (black line) and $C_{org}:P_{tot}$ (blue line) data from Heintzbjerg²⁶ (a) compared with the following marine records from several other studies: (b) Steinbruch Schmidt, Germany²⁷; (c) Kowala, Poland²⁷; (d) Coumiac, France²⁷; and (e) H-32 Core, Iowa, USA⁵⁹. The pulses of the Kellwasser event are indicated by the shaded regions. The placement of the extinction pulses and timing for each site are as established in the referenced studies.

possibility suggested by the model data is that a volcanic event increased atmospheric CO_2 prior to the UKW, but was insufficient in magnitude to drive extinction on its own. Far from being an extinction level event, such an event may have been relatively short in duration, so short that it has not been recorded in the relatively coarse geologic records currently available. A substantial (but not cataclysmic) volcanic event would still have released large quantities of CO_2 . The resultant increase in greenhouse gases could have catalyzed a shift in climate to wetter conditions, thereby driving increased rates of silicate rock weathering, increased carbon sequestration and eventually drawing down atmospheric CO_2 . While the coarse nature of current geologic records provides no direct evidence for short-term CO_2 increases prior to the Kellwasser Events, sedimentary markers and strontium/copper records from Heintzbjerg support the distinct shift in climate conditions from cool and arid to warm and wet²⁶. While these climate shifts could be a result of factors other than CO_2 -induced warming (e.g., orbital forcing²⁶), a large LIP-driven coupled CO_2 /warming event such as that seen during the end-Permian extinction would not necessarily be required to create favorable conditions for plant growth, merely an eruption which elevates atmospheric CO_2 above ambient levels. Atmospheric CO_2 enrichment increases plant growth as well as water use efficiency (i.e., the CO_2 fertilization effect⁶²). Indeed, our model predicts an increase in net primary production on land for the enhanced volcanic degassing scenario accompanying both the LKW and UKW extinction pulses on the order of 2.5 and 6.2 $Gt\ yr^{-1}$ for each, respectively (Extended Data Fig. 1). However, a large-scale eruption such as our modeled volcanic degassing scenario is not required to induce fertilization. CO_2 fertilization has been observed to result in substantial (nearly 30%) increases in plant biomass in experiments on extant temperate ecosystems with CO_2 increases of between 100–300 ppm above ambient concentrations⁶³, levels which fall well inside uncertainty regarding atmospheric CO_2 concentrations in the

Late Devonian. Reduced volcanic degassing could be attributed to regional arc volcanism and perhaps not even associated with a LIP at all. Such a scenario has been proposed for the Late Devonian and could explain both the lack of global evidence for large scale LIP eruption synchronous with the LKW and UKW as well as the lack of large scale CO_2 increases immediately prior to both events^{15,16,38}. The role of regional arc volcanism in environmental calamities is gaining traction and has been invoked as a contributing factor in the end-Permian mass extinction⁶⁴. CO_2 emissions of this magnitude would likely be ephemeral as the resultant expanding forests, increasing rates of silicate rock weathering and ocean sequestration of carbon would quickly return CO_2 levels to background (as well as any associated atmospheric temperature perturbations), leaving no long-term trends recorded in the rock record⁶⁵. While such a muted flux of CO_2 (when compared with that of the end-Permian extinction) is not likely to bring about substantial global temperature or precipitation changes (though there certainly would have been at least minor effects), orbitally induced climate change could account for this discrepancy. This explanation has been invoked by recent studies as a contributing factor in Late Devonian climate instability^{11,26,58,66}. Ma et al. reported the alignment of high orbital eccentricity and obliquity during both the LKW and UKW in two marine sequences in South China⁶⁶. Such an alignment would result in enhanced seasonality, specifically driving warmer and wetter summers which would result in similar favorable conditions for land plant expansion as those invoked above for a LIP eruption scenario⁶⁶. This type of orbitally induced climate change could also explain the climate shifts observed at Heintzbjerg during both the LKW and UKW.

Proliferation of the earliest trees such as cladoxyloids (e.g., *Wattieza*) and archaeopteridaleans (e.g., *Archaeopteris*) has been associated with warmer and wetter conditions as well as periods of increased atmospheric CO_2 concentrations^{65–68}. The spread of cladoxyloids occurred primarily in the Mid Devonian (see

refs. ^{26,65} and references contained therein), and may have been associated with smaller ocean anoxic events²⁶. *Archaeopteris* however, while first-appearing in the Givetian, did not achieve hegemony until the Frasnian. Being the first tree with extensive root systems, stepwise colonization of *Archaeopteris* would have had substantial impacts on regional biogeochemical cycling in the Frasnian²⁶. Regardless of the mechanism for climate change discussed above, a large but transitory increase in atmospheric CO₂ (and associated climate changes) resulting from volcanic degassing, possibly in conjunction with orbitally induced climate fluctuations, may have been sufficient to sustain a rapid expansion of land plants in the late Frasnian. The expansion of land plants, and in particular *Archaeopteris* with its larger and more complex root systems, could have resulted in the observed increases in terrestrial export of phosphorus²⁶. Exported phosphorus would have made its way to the Rheic Ocean, driving anoxia not only in the deeper portions of the basin, but also eutrophication of the shallower margins, partially explaining the collapse of Devonian reef systems observed at the Frasnian–Famennian boundary. A similar mechanism has been proposed as an explanation for the staggered expansion of land plants in the Mid Devonian of New York State, USA⁶⁵ and appears possible in the Devonian Basin in East Greenland as well²⁶. Arens and West⁴⁰ in the development of their press-pulse theory concluded that volcanism (press) must be followed by an additional trigger (pulse) in order to drive mass extinction. Our model, supported by geochemical data, suggests that large scale, but not catastrophic, volcanism served as the “press”, catalyzing atmospheric and climate changes. These changes resulted in substantial environmental stress, but also encouraged plant expansion in East Greenland, subsequently enhancing terrestrial nutrient flux on a massive scale which then provided the “pulse” that tipped the biosphere into mass extinction. The inclusion of orbitally induced climate fluctuations provides the vector for an additional “pulse” which would only have exacerbated the stress on the biosphere and potentially could have strengthened the stress created by land plant expansion. The concurrence between Heintzbjerg and the records from the other sites discussed here showing similar rates of phosphorus export are supportive of the global nature of these events (Fig. 6). The geochemical instability initiated by large scale volcanism combined with the rapid geochemical feedbacks produced by the collective effects of increased rates of silicate rock weathering and land plant expansion would have been sufficient to drive widespread ocean anoxia culminating in mass extinction.

Extinction events are complex systemic responses, and with rare exceptions have seldom been attributed to a single cataclysm. The various theories regarding the initiation of the KW events may each be correct in that they likely contributed to the ecological crisis, although their true timing and sequence clearly need refinement. Our results suggest that neither large scale volcanism nor land plant evolution can be implicated as the sole extinction mechanism in the KW event. Instead, the KW event was probably the timely combination of multiple events ultimately resulting in the collapse of life in Devonian seas. Evidence presented here challenges a single extinction mechanism and demonstrates the need for further work, such as more complex biogeochemical modeling which incorporates both ultimate trigger mechanisms and proximate causes (i.e., press-pulse). Additionally, greater fidelity on the global CO₂ record leading up to, and during, the KW Events as well as more accurate dating of Late Devonian LIPs would greatly aid our understanding of extinction mechanisms and timing. Regardless, only through integration of multiple theories can we hope to bring together the exact timing and sequence of events which culminated in one of the Phanerozoic’s most devastating mass extinctions.

Methods

P/Al and phosphorus accumulation data. P/Al data was taken directly from Smart et al.²⁶ (Fig. 2) and scaled as described below. Due to limitations in the sample repository at the University of Southampton from which the Heintzbjerg samples were sourced, the initiation of the LKW was not covered in the Heintzbjerg sample set. Although the onset of the LKW is not recorded, data from the LKW section that was recorded was used to drive the model as described below. Additionally, without the base of the LKW, Smart et al.²⁶ were unable to establish an age control point at the base of the LKW (nor were they able to establish an age control point for samples in the Famennian). Age control points were however, established for the end of the LKW, base of the UKW and the Frasnian–Famennian boundary as described in Smart et al.²⁶ by recognizing palynozones combined with distinct sedimentary events available at Heintzbjerg. The palynological assemblages at Heintzbjerg were consistent with subzones established for North-west Russia (which falls in the same phytogeographic province as East Greenland) where *Corbulispora vimineus*–*Geminispora vasjamica* is the basal Famennian zone, *Grandispora substuta* is the latest Frasnian and *Auroraspora speciosa* is late Frasnian (pre-UKW)^{69,70} (Fig. 2). Distinct sedimentary events associated with drastic shifts in climate conditions during the LKW and UKW were used to further support the placement of these age control points²⁶. While it should be noted that distinct sedimentological changes by themselves cannot necessarily be used to define a boundary (as their expression may vary depending on location and are also heavily impacted by local sedimentation processes), Smart et al. employ the paleoclimate proxy strontium/copper which is generally corroborative of the sedimentological interpretations²⁶. Here we further build on the age control points established in Smart et al.²⁶ by incorporating a cyclostratigraphic age model to confirm our placement of the end of the LKW, onset of the UKW and Frasnian–Famennian boundary (see below). The concurrence of these three distinct methods lends confidence to our placement of the boundaries at Heintzbjerg. These age control points were used to calculate average sedimentation rates and phosphorus (P) accumulation rates between each of those sections²⁶. Although the P/Al data is informative of terrestrial phosphorus export, P accumulation rate is a more robust parameter from which to gauge phosphorus weathering and subsequent landscape stabilization (see refs. ^{26,71,72}). In the case of the Heintzbjerg study site, these increases in P accumulation were shown to be directly correlated with the presence of deeply rooting land plants such as *Archaeopteris*, suggesting a link between land plant colonization and elevated P export²⁶. In order to use P accumulation data as an input into our model however, it was critical that sedimentation rates, and thus P accumulation rates, be calculated for the entire sequence to capture not only the LKW, but also the post-UKW geochemical response.

Recent refinements in the age of the Frasnian–Famennian boundary from similar sequences^{11,27} make it possible to use relative dating techniques to established estimated ages for the entire sequence based on this anchor point, thus allowing calculation of sedimentation rates and P accumulation rates for the entire Heintzbjerg sequence. The field of astrochronology has long used Milankovitch cycles to gauge the passage of time in sedimentary sequences. Climatic oscillations recorded in the sedimentary record can be tied to changes in the Earth’s orbital parameters. Specifically, the ellipticity of Earth’s orbit (referred to as eccentricity, with periods of 405 kyr, 123 kyr and 95 kyr), tilt (referred to as obliquity, with a modern period of 41 kyr and varying periods in deep time⁷³) and precession (with a modern period of 20 kyr and also varying in deep time⁷³). Meyers⁷⁴ (further refined in ref. ⁷⁵) utilized a statistical optimization method called TimeOpt in the *Astrochron* package in the R platform⁷⁶ in order to correlate climatic changes in the

stratigraphic record with Milankovitch cycles to establish relative age of a sedimentary sequence. We employ a similar approach here, but utilize the timeOptTemplate function which was designed for more complex sedimentation models⁷⁵ which we expected to encounter given the wet/arid climatic shifts noted in the Heintzbjerg sedimentary sequence. The timeOptTemplate function allows the use of proxy or lithology-specific templates which greatly enhance the spectral alignment and overall fit for complex sedimentary sequences. We evaluated the utility of multiple climate-related proxies using this method along with geochemical data from²⁶ ultimately selecting Rb/Sr and Log Ti as proxies which produced the best spectral alignment and overall fit (e.g., ref. ¹¹). Eccentricity periods of 94.9, 98.9, 123.8, 130.7 and 405 kyr⁷⁷ along with precession periodicities for the Devonian of 16.85 and 19.95 kyr⁷³ were utilized. The sedimentation rates estimated using timeOptTemplate were compared with sections calculated by²⁶ and found to be of similar magnitude (Midnatspas average sedimentation rate = 43 cm kyr⁻¹ (see²⁶) compared with 71.9 cm kyr⁻¹ (timeOptTemplate); UKW average sedimentation rate = 272 cm kyr⁻¹ (see ref. ²⁶) compared with 228.6 cm kyr⁻¹ (timeOptTemplate). Age estimates were then determined based on the Frasnian–Famennian boundary (371.870 Ma¹¹) as an anchor point and compared with age estimates for similar published sequences^{11,27}. Using timeOptTemplate estimations, we calculated the base of the UKW of our sequence at 372.06 Ma (compared with 372.00–372.02 Ma based on^{11,27}) and the end of the LKW at 372.49 Ma (compared with 372.45 Ma based on¹¹), a mere 40 kyr difference for each and lending confidence in the validity of the timeOptTemplate results. The concurrence of our cyclostratigraphic age model for Heintzbjerg with those of similar Late Devonian sequences supports our boundary placement here.

Based on the relative confirmation of the timeOptTemplate results, new P accumulation rates were calculated for the entire Heintzbjerg sequence. Once again, these results were compared with those sections calculated in ref. ²⁶ and found to be strikingly similar in overall trends, but notably with somewhat differing magnitudes (Extended Data Fig. 2). The differences in magnitude however, do not change the overall interpretation by Smart et al. ²⁶. Thus, these new P accumulation rates were used as input into our model as described below.

Earth system box model. The basic model design in this study was based on the Carbon Oxygen Phosphorus Sulfur Evolution model^{52,53}, which has been extensively tested and validated against geologic records during the Phanerozoic (e.g., refs. ^{31,52,53}). We incorporate refinements to this model from Ozaki and Reinhard⁵¹ and extend the biogeochemical framework for the seawater carbonate system and global methane (CH₄) cycle without altering the basic behavior of the model. While Ozaki and Reinhard⁵¹ include the mass exchange between the surface system (atmosphere-ocean-crust) and the mantle, we ignore this in this study. We initialized the model at 600 Ma and ran the model forward in time until the end Famennian. Specific model parameters for each experiment are outlined in the following two sections.

Enhanced terrestrial nutrient export scenario. To test the enhanced P export hypothesis, we introduced a forcing factor, f_{pP} , which represents the amplification factor for the terrestrial phosphorus weathering flux:

$$J_P^w = f_{pP} \left(\frac{2}{12} \frac{J_{sil}^w}{J_{sil}^{w*}} + \frac{5}{12} \frac{J_{carb}^w}{J_{carb}^{w*}} + \frac{5}{12} \frac{J_{orgC}^w}{J_{orgC}^{w*}} \right) J_P^{w,*}, J_P^w = f_{pP} \left(\frac{2}{12} \frac{J_{sil}^w}{J_{sil}^{w*}} + \frac{5}{12} \frac{J_{carb}^w}{J_{carb}^{w*}} + \frac{5}{12} \frac{J_{orgC}^w}{J_{orgC}^{w*}} \right) J_P^{w,*}, \quad (1)$$

where J_P^w , J_{sil}^w , J_{carb}^w , and J_{org}^w denote the rates of phosphorus weathering, silicate weathering, carbonate weathering, and the oxidative weathering of organic matter on land, respectively, and * represents the reference value (pre-industrial flux; see refs. ^{51,52}). To assess the uncertainty in the timing and amplitude of pulses in phosphorus weathering, we explored the following different scenarios: (i) In an attempt to reproduce the 2–3‰ positive excursions in $\delta^{13}C$, the following forcing factors were assumed; (LKW) $f_{pP} = 1 \rightarrow 2 \rightarrow 1$ over 372.72–372.54–372.36 Ma. (UKW) $f_{pP} = 1 \rightarrow 2 \rightarrow 1$ over 372.1–371.91–371.73 Ma. (ii) As *i* but decreasing the forcing factor to 1.5 for both the LKW and UKW. (iii) As *i* but decreasing the forcing factor to 1.5 for the LKW only. (iv) f_{pP} based on the P/Al data from Heintzbjerg, Greenland (Fig. 3, left panel), with a scaling factor of 0.5 (see below). (v) f_{pP} based on P accumulation data from Heintzbjerg (Fig. 3, right panel) and applying a scaling factor of 0.15 to account for the hypothesized episodic expansion of land plants as predicted in refs. ^{26,65}, assuming a maximum value of $f_{pP} = 3.35$.

To convert the sedimentary data of P (P/Al or P accumulation rate) into the forcing factor of f_{pP} in (iv) and (v), we first calculate the typical ‘non-event’ value by averaging data between LKW and UKW (Midnatspas Fm.), X_{avg} . Then, f_{pP} is calculated, as follows:

$$f_{pP} = 1 + \frac{X - X_{avg}}{X_{avg}} a, \quad (2)$$

where X denotes the sedimentary data of P (P/Al or P accumulation rate) and a represents the scaling factor. When $a = 1$, f_{pP} (and global P loading flux) simply reflects the variation of P flux observed at Heintzbjerg. But, in this case, our model predicts an extremely large positive excursion of $\delta^{13}C$ (10‰), inconsistent with geologic records. The scaling factor is therefore introduced to represent the relationship between the Heintzbjerg P records to global P export flux. The scaling factor value was tuned so that the model produces a reasonable positive excursion of $\delta^{13}C$ of 2–3‰.

Enhanced volcanic activity scenario. To understand the biogeochemical consequences of the enhanced volcanic activity, we assume that the volcanic activity would have had to occur during the KW events in order to bring about an extinction level event (with current geologic records suggesting the eruption of the Viluy Traps as the most likely culprit). We introduced a forcing factor, f_{LIP} , which is multiplied by the degassing rate of CO₂ via carbonate and organic carbon metamorphisms:

$$J_{carb}^m = f_{LIP} f_G f_C \left(\frac{C}{C^*} \right) J_{carb}^{m,*}, J_{carb}^m = f_{LIP} f_G f_C \left(\frac{C}{C^*} \right) J_{carb}^{m,*} \quad (3)$$

$$J_{org}^m = f_{LIP} f_G \left(\frac{G}{G^*} \right) J_{org}^{m,*}, J_{org}^m = f_{LIP} f_G \left(\frac{G}{G^*} \right) J_{org}^{m,*}, \quad (4)$$

where J_{carb}^m and J_{org}^m denote carbon dioxide (CO₂) degassing flux via metamorphism of sedimentary carbonate (C) and organic carbon (G), respectively (* represent reference values found in⁵²). f_G and f_C represent the forcing factors of degassing flux and pelagic carbonate deposition which are used in the original model. By varying the value of f_{LIP} , we explore the possible impacts of CO₂ degassing rate on global biogeochemistry (Fig. 4): $f_{LIP} = 1 \rightarrow 2 \rightarrow 1$ over 372.72–372.54–372.36 Ma. (UKW) $f_{LIP} = 1 \rightarrow 5 \rightarrow 1$ over 372.1–371.91–371.73 Ma. Here we try and reproduce key changes in the $\delta^{13}C$ record with plausible geological forcing scenarios. While such an increase in CO₂ degassing rates is highly plausible based on reported mercury enrichments concurrent with the KW events^{15,16,54,78}, it is worthy of note that not all mercury records universally support global volcanism^{38,79}, and thus an increase in degassing rate. However, global Paleozoic atmospheric CO₂ records are coarse in nature and may not

necessarily record transient increases in atmospheric CO₂ levels. Transient increases in atmospheric CO₂ may also have been overprinted by resultant feedback mechanisms, preventing their obvious expression in the geologic record.

Data availability

The datasets generated and/or analyzed during the current study are available within the paper, the supplementary information files or available on Figshare (<https://doi.org/10.6084/m9.figshare.23398124.v1>).

Received: 26 October 2022; Accepted: 7 November 2023;

Published online: 29 November 2023

References

- Raup, D. M. & Sepkoski, J. J. Mass extinctions in the marine fossil record. *Science* **215**, 1501–1503 (1982).
- McGhee, G. R. Jr, Clapham, M. E., Sheehan, P. M., Bottjer, D. J. & Droser, M. L. A new ecological-severity ranking of major Phanerozoic biodiversity crises. *Palaeogeogr. Palaeoclimatol. Palaeoecol.* **370**, 260–270 (2013).
- Bond, D., Wignall, P. B. & Racki, G. Extent and duration of marine anoxia during the Frasnian–Famennian (Late Devonian) mass extinction in Poland, Germany, Austria and France. *Geol. Mag.* **141**, 173–193 (2004).
- Carmichael, S. K., Waters, J. A., Koenigshof, P., Suttner, T. J. & Kido, E. Paleogeography and paleoenvironments of the Late Devonian Kellwasser event: A review of its sedimentological and geochemical expression. *Global Planet. Change* **183**, 102984 (2019).
- Joachimski, M. M. & Buggisch, W. Anoxic events in the late Frasnian—Causes of the Frasnian-Famennian faunal crisis? *Geology* **21**, 675–678 (1993).
- Joachimski, M. M. & Buggisch, W. Conodont apatite $\delta^{18}\text{O}$ signatures indicate climatic cooling as a trigger of the Late Devonian mass extinction. *Geology* **30**, 711–714 (2002).
- Chen, D., Qing, H. & Li, R. The Late Devonian Frasnian–Famennian (F/F) biotic crisis: insights from $\delta^{13}\text{C}_{\text{carb}}$, $\delta^{13}\text{C}_{\text{org}}$ and $^{87}\text{Sr}/^{86}\text{Sr}$ isotopic systematics. *Earth Planet. Sci. Lett.* **235**, 151–166 (2005).
- House, M. R. Correlation of mid-Palaeozoic ammonoid evolutionary events with global sedimentary perturbations. *Nature* **313**, 17–22 (1985).
- Buggisch, W. The global Frasnian-Famennian Kellwasser Event. *Geologische Rundschau* **80**, 49–72 (1991).
- Bond, D. P., Zatoń, M., Wignall, P. B. & Marynowski, L. Evidence for shallow-water ‘Upper Kellwasser’ anoxia in the Frasnian–Famennian reefs of Alberta, Canada. *Lethaia* **46**, 355–368 (2013).
- Da Silva, A. C. et al. Anchoring the Late Devonian mass extinction in absolute time by integrating climatic controls and radio-isotopic dating. *Sci. Rep.* **10**, 1–12 (2020).
- Lu, M. et al. Periodic oceanic euxinia and terrestrial fluxes linked to astronomical forcing during the Late Devonian Frasnian–Famennian mass extinction. *Earth Planet. Sci. Lett.* **562**, 116839 (2021).
- Claeys, P., Casier, J. G. & Margolis, S. V. Microtektites and mass extinctions: evidence for a Late Devonian asteroid impact. *Science* **257**, 1102–1104 (1992).
- McGhee, G. R. Jr The ‘multiple impacts hypothesis’ for mass extinction: a comparison of the Late Devonian and the late Eocene. *Palaeogeogr. Palaeoclimatol. Palaeoecol.* **176**, 47–58 (2001).
- Racki, G., Rakociński, M., Marynowski, L. & Wignall, P. B. Mercury enrichments and the Frasnian-Famennian biotic crisis: a volcanic trigger proved? *Geology* **46**, 543–546 (2018).
- Racki, G. A volcanic scenario for the Frasnian–Famennian major biotic crisis and other Late Devonian global changes: more answers than questions? *Global Planet. Change* **189**, 103174 (2020).
- Thompson, J. B. & Newton, C. R. Late Devonian mass extinction: episodic climatic cooling or warming? Paleontology, *Paleoecology and Biostratigraphy*. *Proc. 2nd Int. Symp. Devonian Syst. Memoir* **14**, 29–34 (1988).
- Joachimski, M. M., Pancost, R. D., Freeman, K. H., Ostertag-Henning, C. & Buggisch, W. Carbon isotope geochemistry of the Frasnian–Famennian transition. *Palaeogeogr. Palaeoclimatol. Palaeoecol.* **181**, 91–109 (2002).
- Xu, B. et al. Carbon isotopic evidence for the associations of decreasing atmospheric CO₂ level with the Frasnian-Famennian mass extinction. *J. Geophys. Res. Biogeosci.* **117**, G01032 (2012).
- Huang, C., Joachimski, M. M. & Gong, Y. Did climate changes trigger the Late Devonian Kellwasser Crisis? Evidence from a high-resolution conodont $\delta^{18}\text{O}$ record from South China. *Earth Planet. Sci. Lett.* **495**, 174–184 (2018).
- Wang, X., Liu, S. A., Wang, Z., Chen, D. & Zhang, L. Zinc and strontium isotope evidence for climate cooling and constraints on the Frasnian-Famennian (~372 Ma) mass extinction. *Palaeogeogr. Palaeoclimatol. Palaeoecol.* **498**, 68–82 (2018).
- Averbuch, O. et al. Mountain building-enhanced continental weathering and organic carbon burial as major causes for climatic cooling at the Frasnian–Famennian boundary (c. 376 Ma)? *Terra Nova* **17**, 25–34 (2005).
- Percival, L. M. E. et al. Pulses of enhanced continental weathering associated with multiple Late Devonian climate perturbations: Evidence from osmium-isotope compositions. *Palaeogeogr. Palaeoclimatol. Palaeoecol.* **524**, 240–249 (2019).
- Algeo, T. J., Berner, R. A., Maynard, J. B. & Scheckler, S. E. Late Devonian oceanic anoxic events and biotic crises: “rooted” in the evolution of vascular land plants. *GSA Today* **5**, 45–66 (1995).
- Algeo, T. J. & Scheckler, S. E. Terrestrial-marine teleconnections in the Devonian: links between the evolution of land plants, weathering processes, and marine anoxic events. *Philosophical Transactions of the Royal Society of London. Philos. Trans. R. Soc. Lond. Ser. B Biol. Sci.* **353**, 113–130 (1998).
- Smart, M. S., Filippelli, G. M., Gilhooly, W. P., Marshall, J. E. A. & Whiteside, J. H., Enhanced terrestrial nutrient release during the Devonian emergence and expansion of forests: Evidence from lacustrine phosphorus and geochemical records. *GSA Bull.* **135**, 1879–1898 (2022).
- Percival, L. M. E. et al. Phosphorus-cycle disturbances during the Late Devonian anoxic events. *Global Planet. Change* **184**, 103070 (2020).
- Royer, D. L., Berner, R. A. & Park, J. Climate sensitivity constrained by CO₂ concentrations over the past 420 million years. *Nature* **446**, 530–532 (2007).
- Franks, P. J. et al. New constraints on atmospheric CO₂ concentration for the Phanerozoic. *Geophys. Res. Lett.* **41**, 4685–4694 (2014).
- Royer, D. L. Atmospheric CO₂ and O₂ during the phanerozoic: tools, patterns, and impacts. In *Treatise on Geochemistry*, 2nd ed., 6 (Elsevier, 2014).
- Lenton, T. M., Daines, S. J. & Mills, B. J. COPSE reloaded: an improved model of biogeochemical cycling over Phanerozoic time. *Earth Sci. Rev.* **178**, 1–28 (2018).
- Algeo, T. J. & Ingall, E. Sedimentary Corg: P ratios, paleocean ventilation, and Phanerozoic atmospheric pO₂. *Palaeogeogr. Palaeoclimatol. Palaeoecol.* **256**, 130–155 (2007).
- Berner, R. A. Phanerozoic atmospheric oxygen: new results using the GEOCARBSULF model. *Am. J. Sci.* **309**, 603–606 (2009).
- Zhang, L. et al. An abrupt oceanic change and frequent climate fluctuations across the Frasnian–Famennian transition of Late Devonian: constraints from conodont Sr isotope. *Geological J.* **55**, 4479–4492 (2020).
- Scotese, C. R., Song, H., Mills, B. J., & van der Meer, D. G. Phanerozoic paleotemperatures: the earth’s changing climate during the last 540 million years. *Earth Sci. Rev.* **215**, 103503 (2021).
- Wignall, P. B. *Extinction: a very short introduction* (Oxford University Press, 2019).
- Isozaki, Y. End-Paleozoic mass extinction: hierarchy of causes and a new cosmoclimatological perspective for the largest crisis. In *Astrobiology: From the origins of life to the search for extraterrestrial intelligence*, 273–301 (Springer, 2019).
- Zhao, H. et al. Mercury isotope evidence for regional volcanism during the Frasnian-Famennian transition. *Earth Planet. Sci. Lett.* **581**, 117412 (2022).
- Renne, P. R., Black, M. T., Zichao, Z., Richards, M. A. & Basu, A. R. Synchrony and causal relations between Permian-Triassic boundary crises and Siberian flood volcanism. *Science* **269**, 1413–1416 (1995).
- Arens, N. C. & West, I. D. Press-pulse: a general theory of mass extinction? *Paleobiology* **34**, 456–471 (2008).
- Percival, L. M. et al. Mercury evidence for pulsed volcanism during the end-Triassic mass extinction. *Proc. Natl Acad. Sci.* **114**, 7929–7934 (2017).
- Ernst, R. E., Rodygin, S. A. & Grinev, O. M. Age correlation of large igneous provinces with Devonian biotic crises. *Global Planet. Change* **185**, 103097 (2020).
- Ricci, J. et al. New ⁴⁰Ar/³⁹Ar and K–Ar ages of the Viluy traps (Eastern Siberia): further evidence for a relationship with the Frasnian–Famennian mass extinction. *Palaeogeogr. Palaeoclimatol. Palaeoecol.* **386**, 531–540 (2013).
- Polyansky, O. P. et al. The nature of the heat source of mafic magmatism during the formation of the Vilyui rift based on the ages of dike swarms and results of numerical modeling. *Russ. Geol. Geophys.* **59**, 1217–1236 (2018).
- Meyer-Berthaud, B., Scheckler, S. E. & Wendt, J. *Archaeopteris* is the earliest known modern tree. *Nature* **398**, 700–701 (1999).
- Meyer-Berthaud, B., Soria, A. & Decombeix, A. L. The land plant cover in the Devonian: a reassessment of the tree habit. *Geol. Soc. Lond. Spec. Publ.* **339**, 59–70 (2010).
- Stein, W. E., et al. Mid-Devonian *Archaeopteris* roots signal revolutionary change in earliest fossil forests. *Curr. Biol.* **30**, 421–431 (2020).
- Corlett, H., Feng, J., Playter, T. & Rivard, B. Mapping amorphous SiO₂ in Devonian shales and the possible link to marine productivity during incipient forest diversification. *Sci. Rep.* **13**, 1516 (2023).

49. Zheng, W. et al. Mercury isotope evidence for recurrent photic-zone euxinia triggered by enhanced terrestrial nutrient inputs during the Late Devonian mass extinction. *Earth Planet. Sci. Lett.* **613**, 118175 (2023).
50. Wilder, H. E. I. N. Z. Death of Devonian reefs—Implications and further investigations. *Courier Forschungsinstitut Senckenberg* **172**, 241–247 (1994).
51. Ozaki, K. & Reinhard, C. T. The future lifespan of Earth's oxygenated atmosphere. *Nat. Geosci.* **14**, 138–142 (2021).
52. Bergman, N. M., Lenton, T. M. & Watson, A. J. COPSE: a new model of biogeochemical cycling over Phanerozoic time. *Am. J. Sci.* **304**, 397–437 (2004).
53. Lenton, T. M. et al. Earliest land plants created modern levels of atmospheric oxygen. *Proc. Natl Acad. Sci. USA* **113**, 9704–9709 (2016).
54. Kaiho, K. et al. Coronene, mercury, and biomarker data support a link between extinction magnitude and volcanic intensity in the Late Devonian. *Global Planet. Change* **199**, 103452 (2021).
55. Balter, V., Renaud, S., Girard, C. & Joachimski, M. M. Record of climate-driven morphological changes in 376 Ma Devonian fossils. *Geology* **36**, 907–910 (2008).
56. Joachimski, M. M. et al. Devonian climate and reef evolution: insights from oxygen isotopes in apatite. *Earth Planet. Sci. Lett.* **284**, 599–609 (2009).
57. Dahl, T. W. et al. Low atmospheric CO₂ levels before the rise of forested ecosystems. *Nat. Commun.* **13**, 7616 (2022).
58. De Vleeschouwer, D. et al. Timing and pacing of the Late Devonian mass extinction event regulated by eccentricity and obliquity. *Nat. Commun.* **8**, 2268 (2017).
59. Percival, L. M. et al. Combined nitrogen-isotope and cyclostratigraphy evidence for temporal and spatial variability in Frasnian–Famennian Environmental Change. *Geochem. Geophys. Geosyst.* **23**, e2021GC010308 (2022).
60. Devleeschouwer, X., Herbosch, A. & Pr at, A. Microfacies, sequence stratigraphy and clay mineralogy of a condensed deep-water section around the Frasnian/Famennian boundary (Steinbruch Schmidt, Germany). *Palaeogeogr. Palaeoclimatol. Palaeoecol.* **181**, 171–193 (2002).
61. Larsen, P. H., Olsen, H. & Clack, J. A. The Devonian basin in East Greenland—Review of basin evolution and vertebrate assemblages. In *The Greenland caledonides: evolution of the Northeast Margin of Laurentia*, vol. 202 (Geological Society of America, 2008) p. 273–292.
62. Ueyama, M. et al. Inferring CO₂ fertilization effect based on global monitoring land-atmosphere exchange with a theoretical model. *Environ. Res. Lett.* **15**, 084009 (2020).
63. Walker, A. P. et al. Decadal biomass increment in early secondary succession woody ecosystems is increased by CO₂ enrichment. *Nat. Commun.* **10**, 454 (2019).
64. Edward, O. et al. Timing and provenance of volcanic fluxes around the Permian–Triassic boundary mass extinction in South China: U–Pb Zircon Geochronology, Volcanic Ash Geochemistry and Mercury Isotopes. *Geochem. Geophys. Geosyst.* **24**, e2023GC010912 (2023).
65. Retallack, G. J. & Huang, C. Ecology and evolution of Devonian trees in New York, USA. *Palaeogeogr. Palaeoclimatol. Palaeoecol.* **299**, 110–128 (2011).
66. Ma, K., Hinnov, L., Zhang, X. & Gong, Y. Astronomical climate changes trigger Late Devonian bio- and environmental events in South China. *Global Planet. Change* **215**, 103874 (2022).
67. Brett, C. E., Ivany, L. C., Bartholomew, A. J., DeSantis, M. K. & Baird, G. C. Devonian ecological-evolutionary subunits in the Appalachian Basin: a revision and a test of persistence and discreteness. *Geol. Soc. Lond. Special Publ.* **314**, 7–36 (2009).
68. Retallack, G. J., Hunt, R. R. & White, T. E. Devonian palaeosols and tetrapod habitats in Pennsylvania. *J. Geol. Soc. Lond.* **166**, 1143e1156 (2009).
69. Obukhovskaya, T. G., Avkhimovitch, V. I., Streel, M. & Loboziak, S. Miospores from the Frasnian–Famennian boundary deposits in eastern Europe (the Pripyat Depression, Belarus and the Timan–Pechora Province, Russia) and comparison with western Europe (northern France). *Rev. Palaeobot. Palynol.* **112**, 229–246 (2000).
70. Marshall, J. E., Mangerud, G., Bringu , M. & Bujak, J. Devonian palynoevents in the circum-Arctic region. *Atlantic Geosci.* **58**, 307–328 (2022).
71. Filippelli, G. M. & Souch, C. Effects of climate and landscape development on the terrestrial phosphorus cycle. *Geology* **27**, 171 (1999).
72. Filippelli, G. M. The global phosphorus cycle. *Rev. Mineral. Geochem.* **48**, 391–425 (2002).
73. Berger, A., Loutre, M. F. & Laskar, J. Stability of the astronomical frequencies over the Earth's history for paleoclimate studies. *Science* **255**, 560–566 (1992).
74. Meyers, S. R. The evaluation of eccentricity-related amplitude modulation and bundling in paleoclimate data: an inverse approach for astrochronologic testing and time scale optimization. *Paleoceanography* **30**, 1625–1640 (2015).
75. Meyers, S. R. Cyclostratigraphy and the problem of astrochronologic testing. *Earth Sci. Rev.* **190**, 190–223 (2019).
76. Core Team, R. R. *a language and environment for computing* (R Foundation for Statistical Computing, Vienna, Austria, 2022).
77. Laskar, J., Fienga, A., Gastineau, M. & Manche, H. La2010: a new orbital solution for the long-term motion of the Earth. *Astron. Astrophys.* **532**, A89 (2011).
78. Zhang, J. et al. Mercury anomalies link to extensive volcanism across the Late Devonian Frasnian–Famennian boundary in South China. *Front. Earth Sci.* **9**, 691827 (2021).
79. Liu, Z. et al. Upper Devonian mercury record from North America and its implications for the Frasnian–Famennian mass extinction. *Palaeogeogr. Palaeoclimatol. Palaeoecol.* **576**, 110502 (2021).
80. Scotese, C. R. *Tutorial: PALEOMAP paleoAtlas for GPlates and the paleoData plotter program* (PALEOMAP Project, 2016).

Acknowledgements

We acknowledge the Geological Society of America (Graduate Research Award to M.S.S.), the National Science Foundation (EAR-1850878 to G.F. and W.P.G.), and the Donors of the American Chemical Society Petroleum Research Fund (59949-ND2 to W.P.G. and G.F.) for support of this research. Additionally, this work was partially supported by JSPS KAKENHI (22K18738 to K.O.). C.T.R. wishes to acknowledge the NASA Interdisciplinary Consortia for Astrobiology Research (ICAR) program.

Author contributions

M.S.S., G.F. and W.P.G. designed the study. C.T.R. and K.O. designed the mathematical model and K.O. ran the model. M.S.S. and K.O. interpreted the data. G.F., W.P.G., J.H.W. and J.E.A.M. assisted with interpretations. M.S.S. wrote the manuscript with substantial input from K.O. M.S.S., G.F., W.P.G., C.T.R. and K.O. reviewed the manuscript.

Competing interests

The authors declare no competing interests.

Additional information

Supplementary information The online version contains supplementary material available at <https://doi.org/10.1038/s43247-023-01087-8>.

Correspondence and requests for materials should be addressed to Matthew S. Smart.

Peer review information *Communications Earth & Environment* thanks Grzegorz Racki and the other, anonymous, reviewer(s) for their contribution to the peer review of this work. Primary Handling Editor: Ali nor Lavergne. Peer reviewer reports are available.

Reprints and permission information is available at <http://www.nature.com/reprints>

Publisher's note Springer Nature remains neutral with regard to jurisdictional claims in published maps and institutional affiliations.



Open Access This article is licensed under a Creative Commons

Attribution 4.0 International License, which permits use, sharing, adaptation, distribution and reproduction in any medium or format, as long as you give appropriate credit to the original author(s) and the source, provide a link to the Creative Commons licence, and indicate if changes were made. The images or other third party material in this article are included in the article's Creative Commons licence, unless indicated otherwise in a credit line to the material. If material is not included in the article's Creative Commons licence and your intended use is not permitted by statutory regulation or exceeds the permitted use, you will need to obtain permission directly from the copyright holder. To view a copy of this licence, visit <http://creativecommons.org/licenses/by/4.0/>.

  The Author(s) 2023